



Modular organization of brain resting state networks in chronic back pain patients

Pablo Balenzuela^{1,2*}, Ariel Chernomoretz^{1,2}, Daniel Fraiman^{1,3}, Ignacio Cifre⁴, Carol Sitges⁴, Pedro Montoya⁴ and Dante R. Chialvo⁵

¹ Consejo Nacional de Investigaciones Científicas y Tecnológicas, Buenos Aires, Argentina

² Departamento de Física, Facultad de Ciencias Exactas y Naturales, Universidad de Buenos Aires, Buenos Aires, Argentina

³ Departamento de Matemática y Ciencias, Universidad de San Andrés, Buenos Aires, Argentina

⁴ University Institute of Health Sciences Research IUNICS, University of Balearic Islands, Palma, Spain

⁵ Department of Physiology, David Geffen School of Medicine, University of California at Los Angeles, Los Angeles, CA, USA

Edited by:

Jan G. Bjaalie, University of Oslo, Norway

Reviewed by:

Niels Birbaumer, Institute for Hospitalization and Care Scientific, Italy
Jorge Sepulcre, University of Navarra, Spain

*Correspondence:

Pablo Balenzuela, Av. Cantilo s/n, Departamento de Física, Pabellón 1, Ciudad Universitaria (1428), Buenos Aires, Argentina.
e-mail: balen@df.uba.ar

Recent work on functional magnetic resonance imaging large-scale brain networks under resting conditions demonstrated its potential to evaluate the integrity of brain function under normal and pathological conditions. A similar approach is used in this work to study a group of chronic back pain patients and healthy controls to determine the impact of long enduring pain over brain dynamics. Correlation networks were constructed from the mutual partial correlations of brain activity's time series selected from ninety regions using a well validated brain parcellation atlas. The study of the resulting networks revealed an organization of up to six communities with similar modularity in both groups, but with important differences in the membership of key communities of frontal and temporal regions. The bulk of these findings were confirmed by a surprisingly naive analysis based on the pairwise correlations of the strongest and weakest correlated healthy regions. Beside confirming the brain effects of long enduring pain, these results provide a framework to study the effect of other chronic conditions over cortical function.

Keywords: functional networks, chronic pain, module organization

I. INTRODUCTION

Since the initial work of Eguiluz et al. (2005), complex networks has been widely used to represent functional brain networks. Within this approach, resting state experiments have been analyzed at different scales, either defining nodes as voxels (van den Heuven et al., 2008) or anatomical regions based on a prior automated anatomical labeling (AAL) atlas (Salvador et al., 2005). The organization of resting state brain activity in groups of networks or modules has been studied using different strategies, ranging from univariate analysis as seed correlation (Fox et al., 2005, for example), multivariate linear approaches, as probabilistic independent component analysis (ICA) (Beckmann et al., 2005; Smith et al., 2009) and modular organization in complex networks (Stanberry et al., 2008; Meunier et al., 2009a,b). These analyses has been useful to evaluate the integrity of brain function under normal (Damoiseaux et al., 2006) and pathological conditions (Broyd et al., 2009), including Alzheimer disease (He et al., 2008), schizophrenia (Garrity et al., 2007), and epilepsy (Laufs et al., 2007; Lui et al., 2008), but has not been used in analyzing chronic back pain (CBP) condition.

The experience of pain is usually associated with the activation of a large distributed brain network called the "pain matrix," which includes somatosensory, insular, anterior cingulate and prefrontal cortices, as well as the thalamus (Tracey and Mantyh, 2007). Moreover, previous neuroimaging studies indicate that enduring chronic pain seems to induce a pronounced activation of the pain matrix (Witting et al., 2006) and to alter brain dynamics beyond the feeling of pain itself (Baliki et al., 2008). A recent work (Tagliazucchi et al., 2010) has further reported for the first time alterations in resting state networks of patients with CBP, motivating further work to

evaluate possible global changes in their brain modular organization. This is a significant aim, given that patients with chronic pain suffer from a myriad of symptoms including sleep disturbances, depression, cognitive and attention deficits, etc (Apkarian et al., 2004), whose neurophysiological mechanisms are not yet well understood. Thus, in this paper we use fMRI to identify alterations of brain resting state networks in patients with CBP compared with healthy controls (HC). The modular organization of these networks in both groups is analyzed and significant changes in the communities are contrasted within a pairwise correlations approach.

The paper is organized as follows: Section II describes the experimental conditions. Section II A includes the numerical methods used to construct the functional networks of brain activity and section II B the definition of modularity, node regional roles, and a brief description of the community detection algorithm. Section III describes the community structure of brain functional networks found in both groups together with a detailed analysis of their main features (section III A). Then, a heuristic analysis (section III B) is used to explain the global alterations found in community organization in terms of changes in pairwise correlations. Finally, the identification of the key regions playing a major role in the community organization (section III C) is analyzed. The paper concludes with a discussion of the main alterations found and its consistency with previous findings.

II. MATERIALS AND METHODS

Twelve patients with CBP (29–67 years old, mean \pm SD = 51.2 \pm 11.2) and 12 HC subjects (21–60 years old, mean \pm SD = 40.2 \pm 12.7) participate in the study. Age differences between both groups are not significant ($p < 0.05$). The study was approved by the Northwestern

University IRB committee. All participants were right-handed and completed the Depression and the Anxiety Beck's questionnaires, as well as several pain-related data which have been already published elsewhere (Baliki et al., 2006). As already reported in a previous study the depression and anxiety scores in both groups were far away from pathological criteria, and no group differences were observed on these scores. Participants were scanned following a typical brain resting state protocol (Fox and Raichle, 2007), in which the subject is lying in the scanner and asked to keep their mind blank, eyes closed and avoid falling asleep. Functional magnetic resonance data was acquired in all cases using a 3T Siemens Trio whole-body scanner with echo-planar imaging capability using the standard radio-frequency head coil (scanning parameters were similar to those used in an earlier study, Baliki et al., 2008).

In each subject, a total of 300 images were obtained spaced by 2.5 s. in which the brain oxygen level dependent (BOLD) signal is recorded for each one of the $64 \times 64 \times 49$ sites (so-called voxels of dimension $3.4375 \text{ mm} \times 3.4375 \text{ mm} \times 3 \text{ mm}$). Preprocessing of BOLD signal was performed using FMRIB Expert Analysis Tool (FEAT, Jezzard et al., 2001), <http://www.fmrib.ox.ac.uk/fsl>, involving motion correction using MCFLIRT; slice-timing correction using Fourier-space time series phase-shifting; non-brain removal using BET; spatial smoothing using a Gaussian kernel of full-width-half-maximum 5 mm. Brain images were normalized to standard space with the MNI 152 (average brain image constructed from 152 normal subjects at Montreal Neurological Institute) template using FMRIB's linear image registration tool (FLIRT)¹. Data was band pass filtered (0.01–0.1 Hz) using a 0 lag band pass frequency filter in order to avoid low frequency noise (e.g., scanner drift) and high frequency artifacts (Cordes et al., 2000, 2001). An ICA denoising procedure (Beckmann

and Smith, 2004) consisting in removal edges and high frequency artifacts by linear regression was done using Melodic (PICA). The data was parceled using anatomical regions based on a prior AAL atlas (Tzourio-Mazoyer et al., 2002). This parcellation divides each cerebral hemisphere into 45 anatomical regions. Regional mean time series were estimated for each individual by averaging the BOLD time series over all voxels in each of the 90 regions, which are used to construct the correlation networks.

A. NETWORKS CONSTRUCTION

Inherent to the idea behind computing community's properties is the assumption that brain activity can be described as the flow of activity on a dynamic network (Sporns et al., 2004; Salvador et al., 2005; Eguiluz et al., 2005; Achard and Bullmore, 2007; Bullmore and Sporns, 2009; Meunier et al., 2009b). The first step in this direction is to extract the network from the fMRI data. This is shown schematically in **Figure 1**, where interactions between the ninety regions (Tzourio-Mazoyer et al., 2002) are defined by their mutual co-activity, estimated using partial correlations (**Figure 1A**). Following (Soranzo et al., 2007), the minimum first order partial correlation between X and Y is calculated as,

$$R_c(X, Y) = \min_Z (R(X, Y | Z)), \quad (1)$$

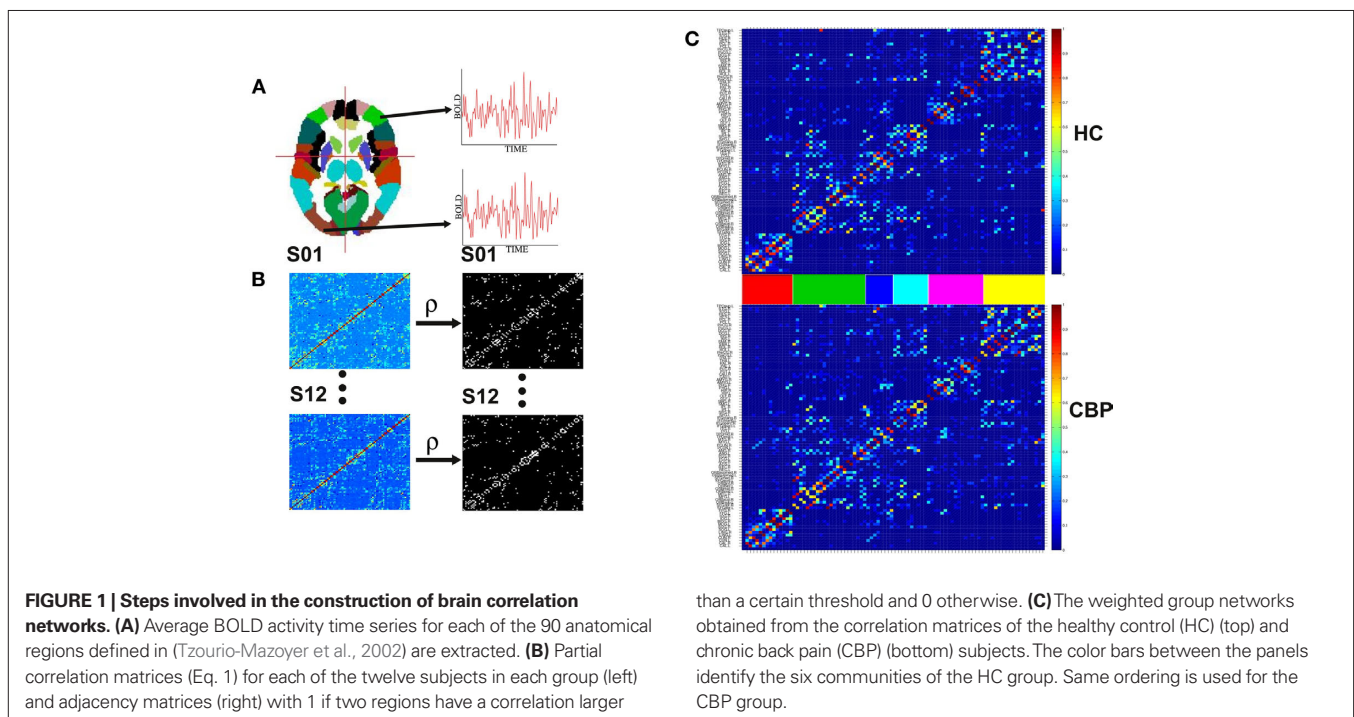
where

$$R(X, Y | Z) = \frac{R(X, Y) - R(Y, Z)}{\sqrt{1 - R(X, Z)^2} \sqrt{1 - R(Y, Z)^2}}, \quad (2)$$

and $R(X, Y)$ is the linear correlation given by

$$R(X, Y) = \frac{\langle X(t)Y(t) \rangle - \langle X(t) \rangle \langle Y(t) \rangle}{\sigma(X(t))\sigma(Y(t))}, \quad (3)$$

¹<http://www.fmrib.ox.ac.uk/analysis/research/flirt/>.



where $\langle \cdot \rangle$ is a temporal average and $\sigma(X(t))$ is the standard deviation of $X(t)$. These calculations result in a 90×90 matrix for each subject (Figure 1B). To define a graph, each matrix is thresholded to create an adjacency matrix A where the a_{ij}^{th} element is either 1 if the value of the partial correlation is greater than a given threshold ρ or 0 otherwise (Figure 1B).

The threshold level is a critical parameter in this kind of analysis. Very small ρ values will produce highly connected networks in which the presence of well defined communities (i.e., group of nodes which are more densely connected amongst them than with the rest of the network) will be hindered. On the other hand, for very high levels of ρ a disconnected network could appear. Since there is not *a priori* scale to choose the ρ 's level, we consider a range of threshold values to get networks with a given fixed number of edges, ranging from $N_L = 100$ up to $N_L = 400$ links ($\rho \sim 0.6-0.9$) as was previously done in (Meunier et al., 2009a).

To compare networks between different groups (i.e., healthy subjects or patients) the data can be collapsed into an average correlation matrix for each group (see Meunier et al., 2009a, for example). This results on a single graph for each group, but the information about variability within each group is lost. To overcome this issue, we compute weighted networks calculated as the average of binary networks of all subjects in the group. The corresponding connectivity matrix reads as:

$$A_{i,j} = \frac{1}{n_p} \sum_{p=1}^{n_p} \Theta(R_C^p(x_i, x_j) - \rho) \quad (4)$$

where n_p is the number of patients in a given group and $\Theta(X)$ is the Heaviside step function ($\Theta(X)$ is 1 if $X \geq 0$ and 0 if $X < 0$). This means that if partial correlations R_C between regions i and j in a given subject p is above threshold, it contributes with $1/n_p$ to the weight of group matrix between regions i and j .

Figure 1C shows the weighted networks estimated from $N_L = 200$ binary networks for both groups. Regions are sorted according to the community structure found in HC group (see Section 2.2) and their location in the adjacency matrix colored to facilitate their identification in subsequent figures. The differences in network community's organization are described in section III.

B. MODULARITY

The definition of a network module is usually given in terms of the subset of graph's nodes which are more densely connected among them than with the rest of the network (Newman and Girvan, 2004). Several algorithms have been proposed to detect these modules in weighted complex networks (Clauset et al., 2004; Newman, 2004; Duch and Arenas, 2005). A common approach is to maximize a quantity that estimates the differences between the actual number of intramodule links and the expected number for the same modules in a randomized network. This quantity, called modularity (Q), can be expressed as:

$$Q = \frac{1}{2m} \sum_{i,j} \left[A_{ij} - \frac{k_i k_j}{2m} \right] \delta(c_i, c_j), \quad (5)$$

where A_{ij} is the adjacency weighted matrix, $m = 1/2 \sum_{i,j} A_{i,j}$ is the number of links of the network and $k_i = \sum_j A_{i,j}$ is the degree of node i (Newman, 2004; Ahnert et al., 2007) and c_i is the community i .

To find communities in brain functional networks we use the algorithm developed by Duch and Arenas (2005), which perform an heuristic search procedure based on extremal optimization (Boettcher and Percus, 2001a,b) to find the network community configuration with the best modularity value.

C. REGION'S ROLES

In a community-structured network, certain nodes might play more important roles than others in the organization of these structures. A fruitful approach to quantify this contribution is to track the intra-modular degree and the participation coefficient of each node (Guimera and Amaral, 2005). The intra-modular degree is a measure of how well connected is a node compared with other nodes of the same community and its z -score can be computed as,

$$z_i = \frac{\kappa_i - \bar{\kappa}_{c_i}}{\sigma_{\kappa_{c_i}}}, \quad (6)$$

with κ_i the intra-modular degree of the i th node, i.e., the number of links of node i to other nodes in its module c_i , $\bar{\kappa}_{c_i}$ as the average of κ_i over all nodes in module c_i and $\sigma_{\kappa_{c_i}}$ the standard deviation of κ_i in c_i .

The participation coefficient quantifies the balance between the intra-module versus inter-module connectivity for a given node. It is defined as

$$P_i = 1 - \sum_{s=1}^{N_M} \left(\frac{\kappa_{ic}}{k_i} \right)^2, \quad (7)$$

where κ_{ic} is the number of links of node i to nodes in module c and k_i is the degree of node i . If all the links of node i fall within its own module, then $\kappa_{ic} = k_i$ and the participation coefficient is 0. On the other hand, if all the links of node i are distributed among all other modules, P_i approaches one.

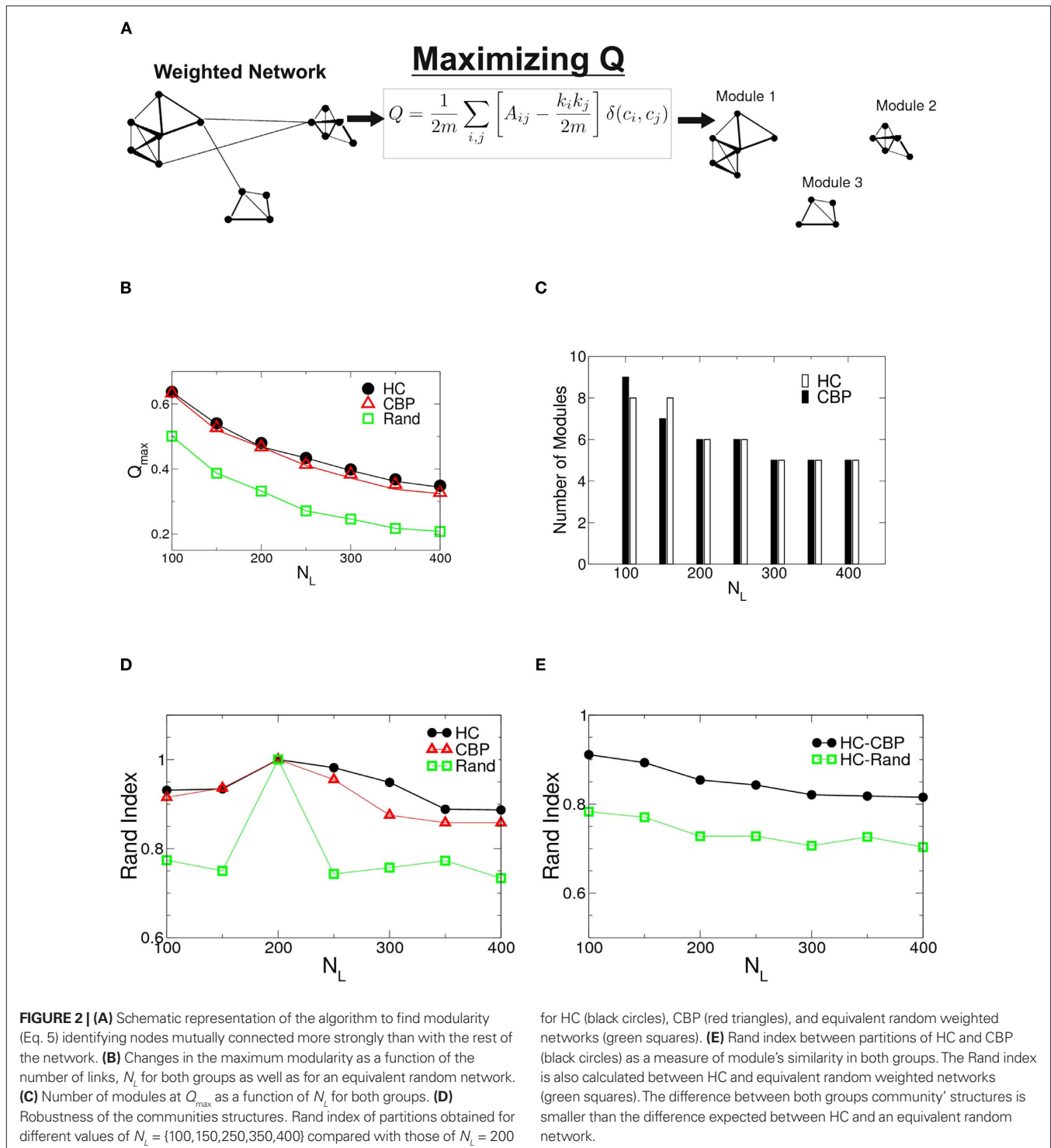
Considering these two definitions, nodes with high intra-modular degree are considered *hubs*, while nodes with high participation coefficients are called *connectors*. These definitions are used here to identify the regions which play key roles in the organization of brain activity at resting state.

III. RESULTS

In this section we will show the results related with the analysis of the structure of functional brain networks. First, we will describe the communities found in both groups, their stability properties and their functional implications. Second, we will analyze which changes in pairwise correlation explains the alterations seen in the CBP communities, and finally we will identify the regions which play key roles in module's organization.

A. COMMUNITIES

The algorithm used to search for partitions which maximizes the network modularity is shown schematically in Figure 2A. For the two groups studied as well as for an equivalent random networks, the maximum modularity values are shown in Figure 2B as a function of $N_L = (N_L, 100-400)$. Notice that both networks show values of Q_{max} larger than their equivalent random networks, implying a highly modular structure. Although Q_{max} depends on N_L , no significant differences were found between HCP and CBP, for any



given N_L . The number of detected modules as a function of N_L is shown in **Figure 2C**. The number of communities stabilizes for $N_L \geq 200$ and is similar for both groups.

To further investigate possible differences between groups, the sets of modules found at Q_{max} were compared, using the Rand index (RI) (Rand, 1971). The RI is a coefficient that quantifies the percentage of agreement between two partitions (X and Y) of a given

set of elements. Thus, $RI = 1$ if both partitions X and Y are exactly the same (i.e., they have the same quantity of modules and the same integrants in each one) and $RI = 0$ if they are completely different.

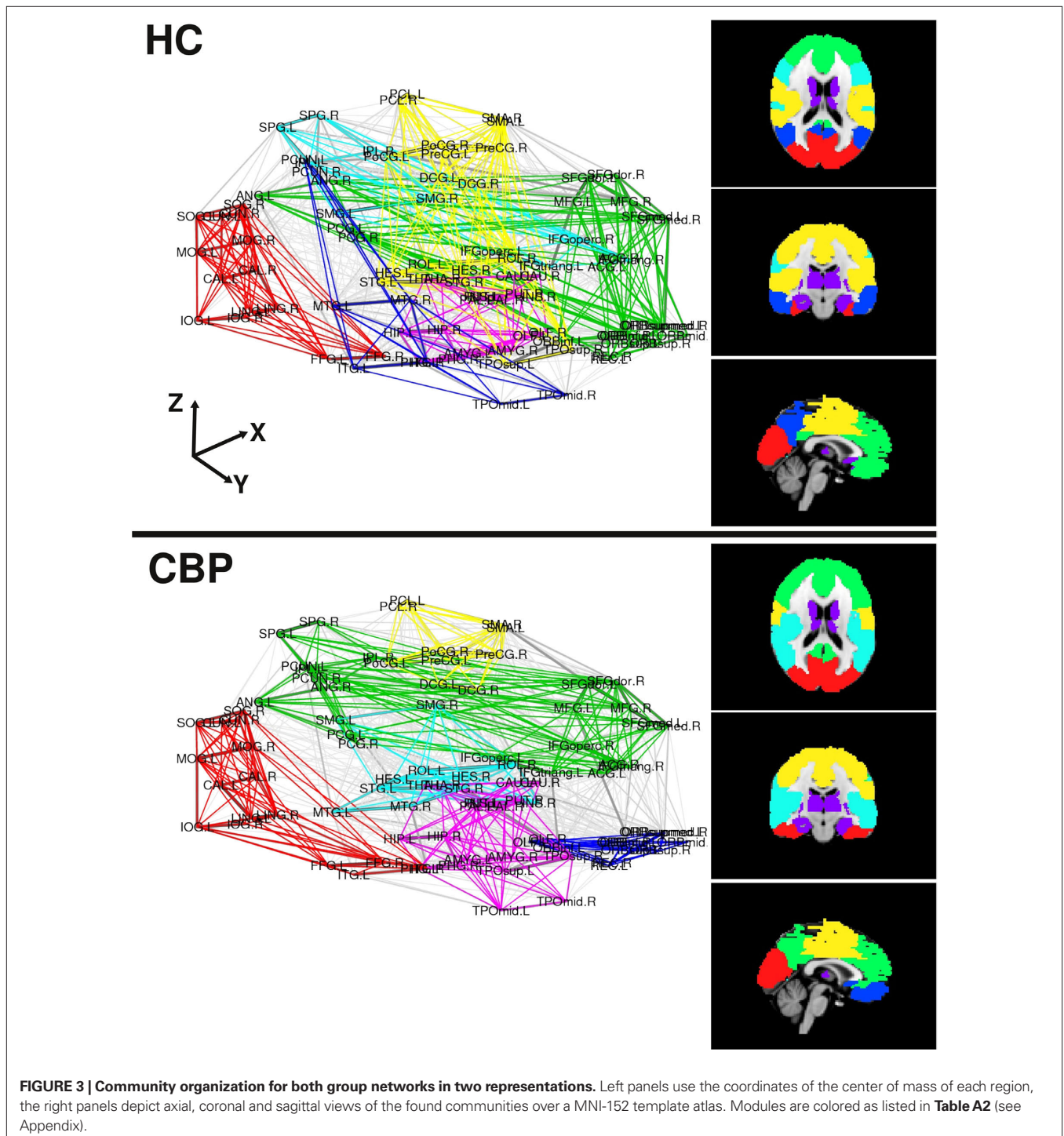
In **Figure 2D** we shown the calculated RI between networks of different N_L with the one corresponding to $N_L = 200$ for HC, CBP, and a random realization. No major changes in community organization

for brain networks is observed as a function of N_L , but large changes are shown in equivalent random networks. This result suggests that the observed structures are a robust feature of the brain networks.

Figure 2E shows the RI between HC and CBP partitions (black circles) as a function of N_L , with the RI calculated between HC and a random equivalent network (green diamond). The differences found between HC and CBP are much smaller than those expected between HC and equivalent random networks. These results suggest

that more detailed analysis is needed to identify potential differences between control subjects and patients. In order to do this we will restrict further analysis to networks with a fixed N_L . Since the number of communities at Q_{\max} stabilizes for $N_L = 200$, such value was chosen as representative.

The modular structure in which the brain network organizes (for $N_L = 200$) are shown in **Figure 3** depicted in two ways. In the left panels we use an anatomical representation with the coordinates of



the center of mass of each region. Right panels display a brain representation in axial, coronal, and sagittal views of found communities over a MNI-152 template atlas. We can observe that both, the HC and the CBP group networks, show a structure formed by up to six communities which are listed in **Table A2**, along with the membership for each community (see Appendix). Abbreviations used for brain regions (as in Salvador et al., 2005) can be found in **Table A1** (see Appendix).

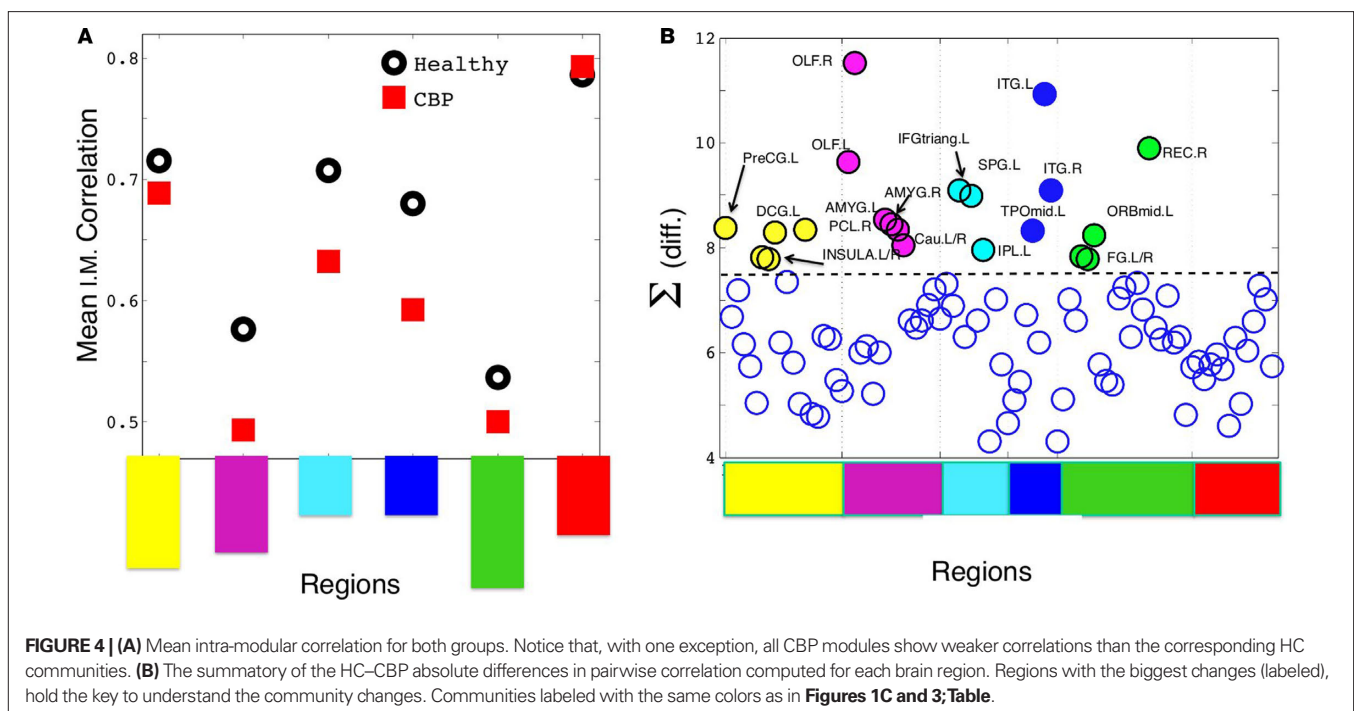
A detailed analysis of these findings can be summarized as follows (see also **Figure A1** in Appendix): The first community (red/visual) involves several regions of the lateral and medial visual pathways (calcarine, cuneus, lingual, and occipital gyri) and could be related to the visual resting state network postulated by Beckmann et al. (2005). This community appears to extend to the inferior temporal gyrus in CBP, but not in HC. A second community (green/fronto-medial) was mainly composed of several frontal regions (superior and inferior frontal gyrus, orbito-frontal cortex), as well as anterior cingulate and angular gyri. This community could be related to two resting state networks: the default mode (DMN) and the executive control networks (Beckmann et al., 2005). This community appears to be altered in CBP patients, because it extends to the precuneus and the medial frontal cortex in CBP patients, but does not include the orbito-frontal cortex as it occurs in HC. The third community (blue/parieto-temporal) is formed by the precuneus and the temporal lobes in HC, displaying similarities to Beckmann's DMN. This community extends to the orbito-frontal cortex in CBP patients, but not in HC. The fourth community (light blue/fronto-parietal) involves regions from the inferior frontal cortex, the superior parietal and the supramarginal gyrus, and could be associated with two resting state networks: the auditory system and the dorsal visual stream (Beckmann et al., 2005). This community extends to the insula in CBP patients, but not in HC.

The fifth community (magenta/subcortical) is comprised by subcortical regions, such as hippocampus, thalamus, basal ganglia, and amygdala. No differences between groups appeared in the module membership of this community. The last community (yellow/sensorimotor) includes the sensorimotor cortices as well as other regions of the pain network such as cingulate gyrus and insula (Zaki et al., 2007). This community appears to be altered in CBP patients because it does not include the insula and the posterior portion of the cingulate gyrus as it occurs in HC. A side by side comparison between HC and CBP communities and Beckmann's resting state networks can be found in **Figure A1** of Appendix.

B. PAIRWISE CORRELATIONS SUFFICE TO EXPLAIN COMMUNITIES CHANGES?

The results displayed in **Figure 3** show that the observed changes in modular organization are basically of three types: (I) there are communities that split into two or more subgroups, (II) there are modules that fuse together forming a single community, and (III) nodes are adsorbed into other communities, and some communities disappear. Admitting that these changes can be brought about by a complex combination of factors, we test here for the simplest of all cases, which is that linear bivariate correlation changes can be sufficient to explain any of the three types of communities changes.

Thus we re-analyze the interactions between nodes through pairwise correlations. An important point is that we start taking the community partition of the HC (**Figure 3** top) as a reference frame and compute the mean intra-modular correlation, \bar{r}_{IM} , for each of the communities defined in this reference HC group. The idea is that \bar{r}_{IM} should estimate the strength of the bonds holding together the communities, and that changes should occur preferentially in weakly coupled modules. **Figure 4A** shows \bar{r}_{IM} for each



of the six communities in both groups. It can be seen that CBP patients exhibit a mean intra-modular correlation smaller than control subjects, with the exception of the Posterior module (red). This is consistent with the expectation that communities with weakest correlations should be the ones more easily segregated by potential pathological changes in the interactions.

Thus we focus at the weight (interaction) changes within each community. The largest changes respect to the HC hold the key to understand all the community alterations. We start by computing the summatory of correlations for each node (plotted in **Figure 4B**) and inspecting the nodes exhibiting the largest (absolute) change in its correlations. Then, we look whether these changes can explain directly any of the structural changes observed in a given community.

The corresponding observed changes, as listed below (see **Figure 5**):

- The parieto-temporal community (Coded blue in HC, **Figure 5A**) is not present in CBP. In this module all the pair correlations have decreased (range $[-0.2, -0.1]$) in CBP, breaking this structure apart. Larger correlation levels observed in CBP than in HC between inferior temporal gyrus (ITG) and lingual (LING), fusiform (FFG), and inferior occipital gyrus (IOG) (+0.15) result in the former (ITG) being included in the posterior community (red).
- The fronto-medial (green) community observed in HC splits in two subgroups: a new CBP (orbito-frontal, blue) community is created and the fronto-medial CBP community (green) is reorganized, (see **Figure 5B**). These changes can be explained by the increased interaction between olfactory (OLF), the orbital part of the superior frontal gyrus (ORBsup) and the gyrus rectum (REC) (+0.16) in CBP. Simultaneously the correlation between the orbital part of the middle frontal gyrus (ORBmid) and angular (ANG), middle frontal (MFG), and anterior cingulate gyrus (ACG) decreased (-0.12). This two opposite behaviors give rise to a mean intra-modular correlation that do not change considerably in CBP.
- The same type of behavior can be observed for the Sensorimotor HC community (yellow, **Figure 5C**). In this case, the interaction between the insula and the precentral gyrus (PreCG), the paracentral lobule (PCL), and superior temporal gyrus of temporal pole (TPOsup) are lower in CBP than in HC (-0.13). In addition, the interactions between rolandic operculum, supplementary motor area (SMA) and precentral gyrus (PreCG) are decreased (-0.12), whether correlations between insula and Heschl gyrus in CBP are increased (+0.11).
- The fronto-parietal (light-blue) community observed in HC is adsorbed by the fronto-medial module in CBP (**Figure 5D**), mainly because the interaction between superior parietal (SPG) and supramarginal (SMG) has increased (+0.15).
- In addition, the supramarginal (SMG) region is left apart from the fronto-parietal HC module in CBP (**Figure 5E**). This happens because the interaction between this and inferior parietal (IPL), the opercular part of the middle frontal gyrus (IFGoperc) and the triangular part of the inferior frontal gyrus (IFGtriang) is decreased (-0.14). In this case all the

regions involved in the new community have increased their internal interactions (superior temporal, supramarginal and middle temporal gyrus, insula, and Heschl operculum).

The mentioned arguments show that the changes observed in the CBP networks can be explained by looking at the pairwise interaction changes within each community and focusing on the largest correlation changes respect to the HC. At some point this is to be expected as the algorithm uses precisely these correlations when it assigns each node to a given community.

C. HUBS AND CONNECTORS

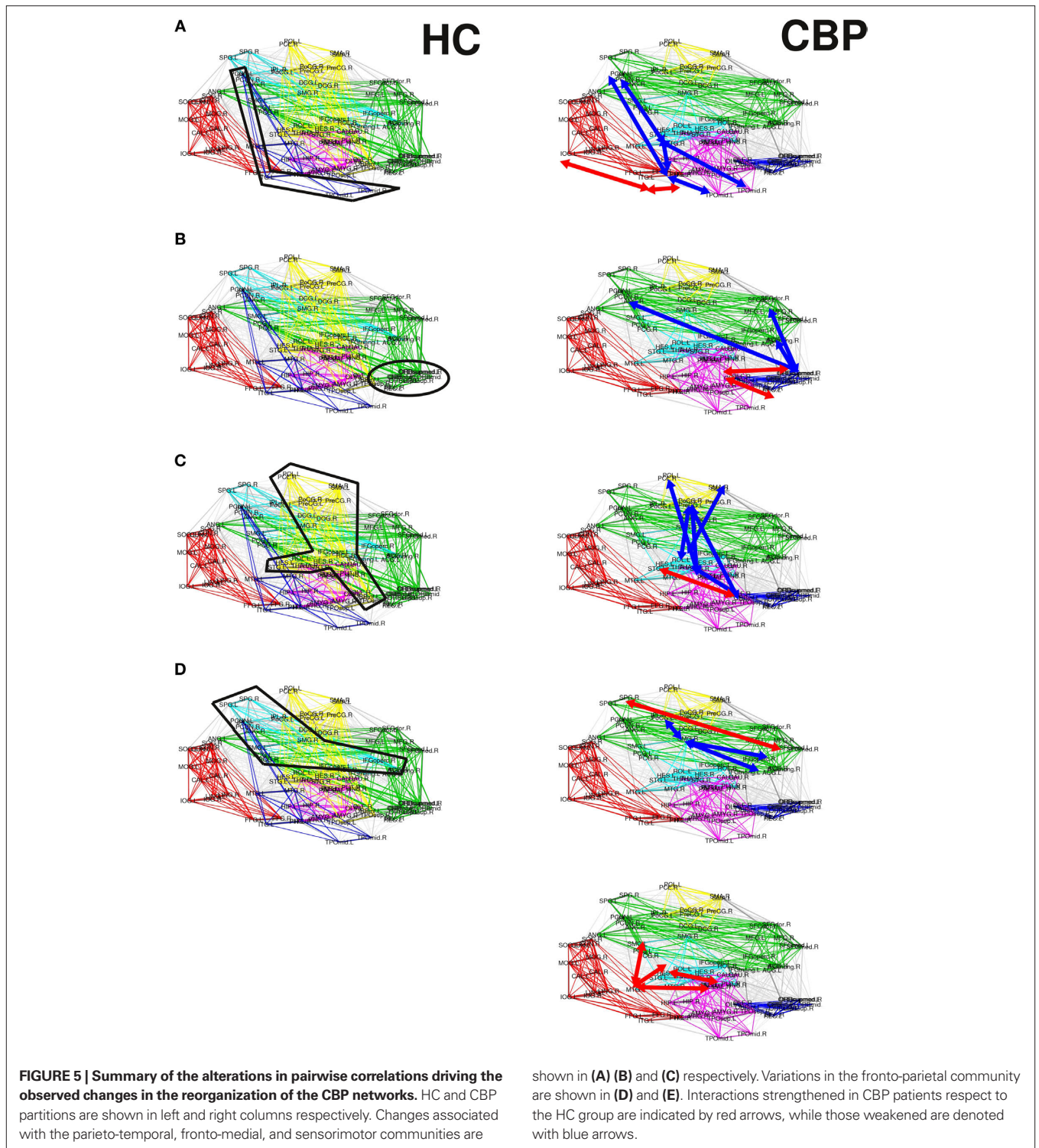
The results discussed in the previous section show that both CBP and HC networks are structured in the same number of communities, although they show notorious differences in organization and region's membership. This produces that, within these communities, certain key regions present different connectivity. To further quantify these differences, the z -score of the intra-modular degree (z_i) and the participation coefficient (P_i) of each node were computed (e.g., Eqs. 6 and 7). This technique allows the labeling in each case of hubs and connectors for each module as it is presented in the top panels of **Figure 6** (see names for each region further detailed in **Table 1**).

The location of hubs and connectors provide clues about the key players in each module organization, thus it is important to study the changes in role of these nodes between the groups. This is plotted in the bottom panels of **Figure 6** for the intra-modular degree and participation coefficient of Healthy Controls $z_{i,(HC)}$ and $P_{i,(HC)}$ versus Chronic Back Pain patients, $z_{i,(CBP)}$ and $P_{i,(CBP)}$. If there were no changes in z_i and P_i , all points should collapse in the diagonal, thus, distance from the diagonal can be interpreted as a measure of region's role change. In the plot, those regions whose change in z_i or P_i are more than two standard deviations are highlighted. Concerning hubs, note that inferior temporal gyrus (ITG.L and ITG.R), superior frontal gyrus, medial orbital (ORBsupMed.R), middle temporal gyrus (MTG.R) and superior frontal gyrus, medial (SFGmed.R) are regions with high intra-modular degree in HC and low intra-modular degree in CBP patients. Superior frontal gyrus, orbital part (OrbSup.L) is a region with high intra-modular degree in CBP and low in HC. Concerning connectors, caudate (CAU.R), superior frontal gyrus, medial orbital (ORBsupMed.R), superior frontal gyrus, medial (SFGmed.R) and anterior cingulate, and paracingulate gyri (ACG.L) are regions whose participation coefficient increase notoriously in CBP respect to HC groups.

For any given node, changes in its z_i or P_i value could arise basically due to two mechanisms: local changes, i.e., when there are changes in its own connectivities (by increasing or decreasing the number of links with the rest of the network) or global changes, i.e., due to changes in the mean intra-modular degree by alterations in other connections or by a change in module memberships. This is demonstrated by the results in **Table 2** which shows the degree of these regions and compares with $\langle k_i \rangle$ of regions who belong to.

IV. DISCUSSION

The major aim of the present study was to examine the modular organization of functional brain networks in CBP. To characterize the modularity of these complex networks, we applied tools from



graph theory to BOLD time series obtained from resting fMRI. The present findings were derived from purely data driven analyses and confirmed by a heuristic approach using pairwise correlations. Based on previous evidence showing extensive alterations of brain dynamics in chronic pain patients (Baliki et al., 2006, 2008; Geha et al., 2008; Tagliazucchi et al., 2010), we hypothesized that topological properties of these functional brain networks (i.e., number and components of

the modules, intra-modular degree, participation coefficient of the nodes) should be altered as a consequence of persistent pain. Our results revealed significant group differences in the modular organization of several brain resting state networks, rather than global changes of brain modularity. Basically, we observed that HC and CBP patients differed in the connectivity of frontal lobes and anterior cingulate gyrus, which are usually involved in the default mode resting

Table 1 | Regions identified as hubs or connectors for each of the communities in both groups.

Module	Hub	Connector
HC		
Visual	Superior occipital gyrus (SOG.R)	Fusiform gyrus (FFG.L)
Fronto-medial	Superior frontal gyrus, medial (SFGmed.R)	Inferior frontal gyrus, orbital part (ORBinf.L)
Parieto-temporal	Middle temporal gyrus (MTG.R)	Precuneus (PCUN.L)
Fronto-parietal	Inferior parietal (IPL.L)	Superior parietal (SPG.L)
Subcortical	Hippocampus (HIP.R)	Caudate nucleus (CAU.L)
Sensorimotor	Supplementary motor area (SMA.R)	Superior temporal gyrus (TPOsup.L)
CBP		
Visual	Fusiform gyrus (FFG.R)	Inferior temporal gyrus (ITG.L)
Fronto-medial	Superior frontal gyrus, dorsolateral (SFGdor.L)	Superior parietal gyrus (SPG.R)
Orbito-frontal	Superior frontal gyrus, orbital part (ORBsup.L)	Inferior frontal gyrus, orbital part (ORBinf.L)
Fronto-parietal	Superior temporal gyrus (STG.L)	Middle temporal gyrus (MTG.R)
Subcortical	Hippocampus (HIP.R)	superior temporal gyrus (TPOsup.R)
Sensorimotor	Supplementary motor area (SMA.R)	Median cingulate and paracingulate gyri (DCG.R)

Table 2 | Changes in node's role.

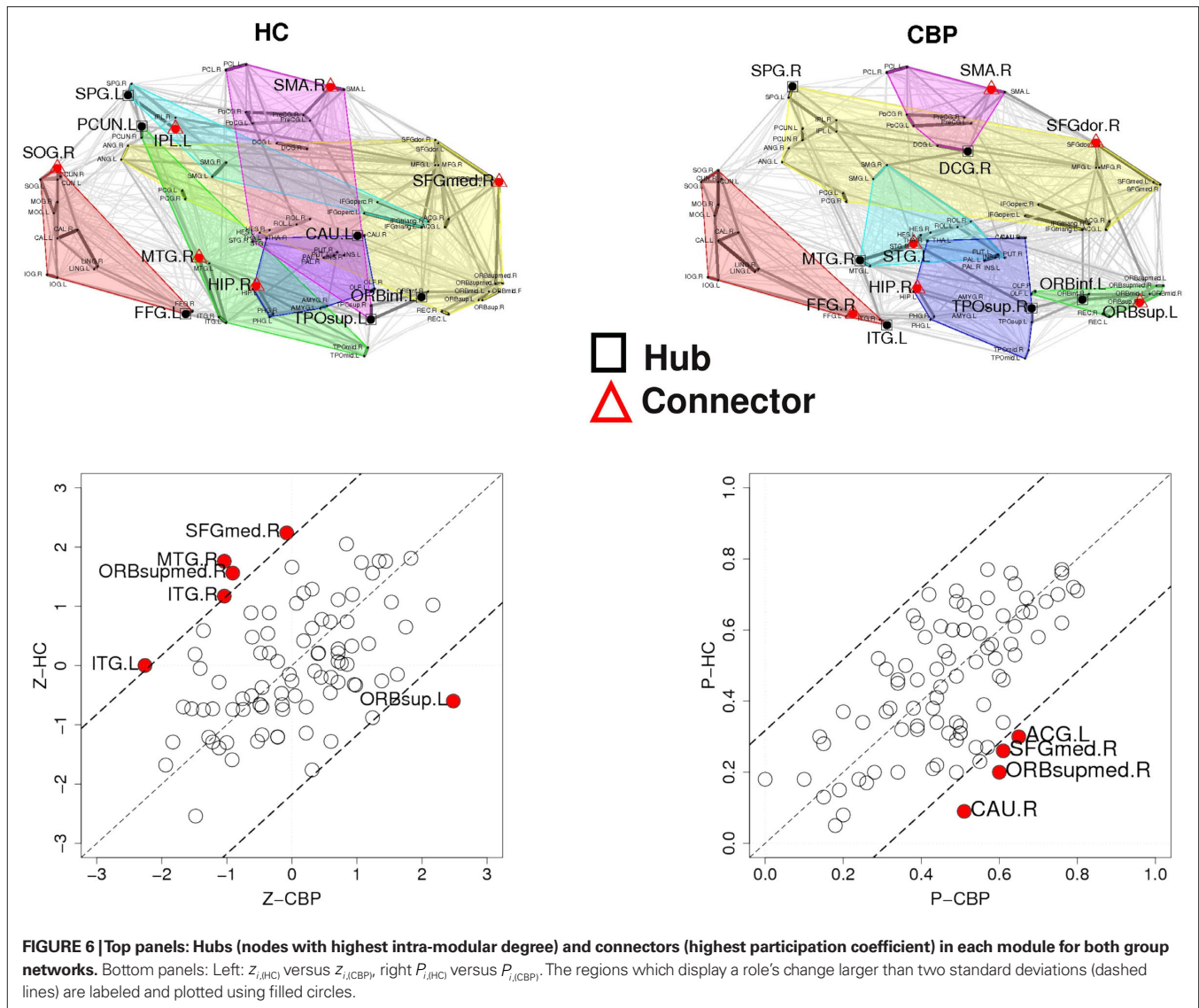
Region	HC			CBP			Type
	k_i	Module	$\langle k_i \rangle_{\text{Module}}$	k_i	Module	$\langle k_i \rangle_{\text{Module}}$	
ITG.L	6.50	Parieto-temporal	2.33	4.25	Visual	3.20	*
ITG.R	7.75	Parieto-temporal	2.33	6.00	Visual	3.20	*
OrbSupMed.R	4.67	Fronto-medial	3.21	3.92	Orbito-frontal	2.40	*
MTG.R	7.17	Parieto-temporal	2.33	7.42	Fronto-parietal	3.14	*
OrbSup.L	3.92	Fronto-medial	3.21	4.33	Orbito-frontal	2.40	*
CAU.R	1.75	Subcortical	2.40	2.42	Subcortical	2.58	†
ACG.L	3.92	Fronto-medial	3.21	5.33	Fronto-medial	3.05	†
SFGmed.R	5.42	Fronto-medial	3.21	5.17	Fronto-medial	3.05	•

Different symbols indicate: *, global changes produced by a switch in module membership; †, local changes due to increment in number of connections of the node; •, changes due to reorganization of links from inter-module links to intra-module links. The node's degree and the mean module degree are also listed.

state network and pain processing. To our knowledge, this is the first report analyzing in detail the structure of these functional brain networks in CBP patients. Indeed, we found that functional brain networks in both healthy and CBP patients were well described by six different communities of modules: Visual (com1), fronto-medial (com2), parieto-temporal (com3), fronto-parietal (com4), subcortical (com5), and sensorimotor (com6). Moreover, it was observed that the modular organization of the functional brain networks in HC was in line with previous studies (Meunier et al., 2009a,b), describing a posterior community (similar to our visual community), a central community (including the sensorimotor and the subcortical communities), and an additional community involving frontal and cingulate cortices as well as the temporal lobes (similar to our fronto-medial and parieto-temporal communities). As a further validation of our approach, we demonstrated that our visual, fronto-medial, parieto-temporal, and fronto-parietal communities were quite similar to the visual, default mode, executive control, and auditory resting state networks (Beckmann et al., 2005), respectively.

Differences between healthy subjects and CBP patients were mainly characterized by a reorganization of fronto-medial, parieto-temporal, fronto-parietal, and sensorimotor communities involving

frontal and temporal structures, as well as sensorimotor cortex, basal ganglia, insula, and anterior cingulate cortex (ACC). Basically, this reorganization implied a change in the module membership of the orbito-frontal cortex, the insula, and the posterior portion of the cingulate gyrus, which are involved in affective and cognitive processing, as well as in somatosensory integration. In addition, we found that caudate nucleus and ACC displayed a high inter-modular connectivity in CBP patients as compared with HC. The ACC has been identified as a key brain region in pain processing, responsible for the integration of sensory, attentional, emotional, and motivational aspects of pain; whereas the caudate nucleus participates in pain processing in sync with the ACC and several regions of the prefrontal cortex (Oshiro et al., 2009). Thus, it appears that chronic pain might be associated with changes in the modular organization and with an increased functional correlation of brain regions involved in processing and integration of sensory, affective, and cognitive components of pain. These findings are consistent with previous reports, showing that enduring pain might disrupt the functional connectivity of cortical regions of the DMN with the insula and the middle frontal gyrus (Baliki et al., 2008; Tagliazucchi et al., 2010), key regions which appear to be implicated in internally generated thought processes (Raichle



et al., 2001) and to play an important role in the evaluation of pain intensity and other somatic signals (Critchley et al., 2004). Moreover, it has been reported that irrespective of the location, nature or course of the different pain syndromes, chronic pain patients exhibit significant reductions of gray matter in cingulate cortex, orbito-frontal cortex, and insula (May, 2008). Accordingly, it seems reasonable that persistent, emotionally laden, self-reflective thoughts as it occurs in chronic pain states might have led to disrupt the modular organization of insula and orbito-frontal cortex and to increase the number of connections of ACC with the rest of the brain.

Our results show an organization comprising the same number of modules, and when changes were detected, they were well explained by straightforward pairwise changes in the linear correlation between a few nodes. Although caution should be always exercised, the fact that pairwise correlations were sufficient to explain global changes, suggests that correlations between a small number of key regions have a chance to be informative about the functional brain connectivity. Another implication of the present

results relates to the physical substrate sustaining these dynamical changes, in particular since it has been previously described that chronic pain may elicit relevant changes in white and gray matter (Geha et al., 2008; May, 2008). These findings are consistent with the alterations in correlations described here, but further studies are needed to establish the validity and extent of the functional and structural relation. If proven true it will reinforce the idea that the stressful experience of enduring pain over many years could by itself modify adaptive synaptic connections, reshaping the connectivity of the subnetworks studied in the present study.

The present study has several limitations. An important one is the underlying assumption that chronic pain patient's brain is altered by the disease. Although this is a reasonable hypothesis it is yet far from proven and, in addition, even if there are alterations, still is unknown how large could be the individual variability. In other words, it is not yet known up to which point the potential changes in cortical dynamics in each individual are consistent across the patient's group, such that it can be detected by the kind of group average

analyses performed here. Another important limitation is the common assumption considering the ninety anatomically defined brain areas as representing the centerpieces of a large-scale brain network. This is a good simplifying approach, that facilitates and compresses information, but it could be limiting our ability to detect differences between groups. One of the reasons is that regions selected by this method, despite covering very different sizes of cortical territories are all being equalized when considered as a single node in a network. Finally, another factor to consider is that the components obtained from an anatomical parcellation method do not necessarily mirror the dynamical components of brain activity as is shown in **Figures A1 and A2** of Appendix where communities found in this work were compared with networks obtained from principal component analyses (as in Beckmann et al., 2005).

In summary, the study of brain correlation networks revealed an organization of up to six communities with similar modularity in both healthy and chronic pain groups. These differences

appeared in the membership of key communities of frontal and temporal regions and confirmed by a surprisingly naive analysis based on pairwise correlations of the strongest and weakest correlated regions in HC. Besides confirming the brain effects of long enduring pain, our results provide a framework for studying the effects of other chronic conditions on functional brain networks.

ACKNOWLEDGMENTS

The authors thank the patients and the healthy volunteers for their participations in the study. Work supported by NIH NINDS of USA, grant No. NS58661, by CONICET (grant No. PIP0802/10 and PIP0087), MinCyt (Grant No. 863) and University of Buenos Aires (grant No. UBACyT X-404), Argentina and by Spanish Ministry of Science and European Funds FEDER (grant No. SEJ2007-62312). Funding for data collection was provided by grant No. NS35115 (awarded to A.V. Apkarian) by NIH NINDS.

REFERENCES

- Achard, S., and Bullmore, E. T. (2007). Efficiency and cost of economical brain functional networks. *PLoS Comput. Biol.* e17. doi: 10.1371/journal.pcbi.0030017.
- Ahnert, S. E., Garlaschelli, D., Fink, T. M. A., and Caldarelli, G. (2007). Ensemble approach to the analysis of weighted networks. *Phys. Rev. E* 76, 016101–016105.
- Apkarian, A. V., Sosa, Y., Krauss, B. R., Thomas, P. S., Fredrickson, B. E., Levy, R. E., Harden, R., and Chialvo, D. R. (2004). Chronic pain patients are impaired on an emotional decision-making task. *Pain* 108, 129–136.
- Baliki, M. N., Chialvo, D. R., Geha, P. Y., Levy, R. M., Harden, R. N., Parrish, T. B., and Apkarian, A. V. (2006). Chronic pain and the emotional brain: specific brain activity associated with spontaneous fluctuations of intensity of chronic back pain. *J. Neurosci.* 26, 12165–12173.
- Baliki, M. N., Geha, P. Y., Apkarian, A. V., and Chialvo, D. R. (2008). Beyond feeling: chronic pain hurts the brain, disrupting the default-mode network dynamics. *J. Neurosci.* 28, 1398–1403.
- Beckmann, C. F., DeLuca, M., Devlin, J. T., and Smith, S. M. (2005). Investigations into resting-state connectivity using independent component analysis. *Philos. Trans. R. Soc. Lond. B. Biol. Sci.* 360, 1001–1013.
- Beckmann, C. F., and Smith, S. M. (2004). Probabilistic independent component analysis for functional magnetic resonance imaging. *IEEE Trans. Med. Imag.* 23, 137–152.
- Boettcher, S., and Percus, A. G. (2001a). Optimization with extremal dynamics. *Phys. Rev. Lett.* 86, 5211–5214.
- Boettcher, S., and Percus, A. G. (2001b). Extremal optimization for graph partitioning. *Phys. Rev. E* 64, 026114–026126.
- Broyd, S. J., Demanuele, C., Debener, S., Helps, S. K., James, C. J., and Sonuga-Barke, E. J. S. (2009). Default-mode brain dysfunction in mental disorders: a systematic review. *Neurosci. Biobehav. Rev.* 33, 279–296.
- Bullmore, E. T., and Sporns, O. (2009). Complex brain networks: graph-theoretical analysis of structural and functional systems. *Nat. Rev. Neurosci.* 10, 186–198.
- Clauset, A., Newman, M. E. J., and Moore, C. (2004). Finding community structure in very large networks. *Phys. Rev. E* 70, 066111–066116.
- Cordes, D., Haughton, V. M., Arfanakis, K., Carew, J. D., Turski, P. A., Moritz, C. H., Quigley, M. A., and Meyerand, M. E. (2001). Frequencies contributing to functional connectivity in the cerebral cortex in “resting-state” data. *Am. J. Neuroradiol.* 22, 1326–1333.
- Cordes, D., Haughton, V. M., Arfanakis, K., Wendt, G. J., Turski, P. A., Moritz, C. H., Quigley, M. A., and Meyerand, M. E. (2000). Mapping functional related regions of brain with functional connectivity MR imaging. *Am. J. Neuroradiol.* 21, 1636–1644.
- Critchley, H. D., Wiens, S., Rotshtein, P., Ohman, A., and Dolan, R. J. (2004). Neural systems supporting interoceptive awareness. *Nat. Neurosci.* 7, 189–195.
- Damoiseaux, J. S., Rombouts, S. A. R. B., Barkhof, F., Scheltens, P., Stam, C. J., Smith, S. M., and Beckmann, C. F. (2006). Consistent resting-state networks across healthy subjects. *Proc. Natl. Acad. Sci. U.S.A.* 103, 13848–13853.
- Duch, J., and Arenas, A. (2005). Community detection in complex networks using extremal optimization. *Phys. Rev. E* 72, 027104–027107.
- Eguiluz, V. M., Chialvo, D. R., Cecchi, G., Baliki, M., and Apkarian, A. V. (2005). Scale-free brain functional networks. *Phys. Rev. Lett.* 94, 018102–018105.
- Fox, M. D., Snyder, A. Z., Vincent, J. L., Corbetta, M., van Essen, D. C., and Raichle, M. E. (2005). From the cover: the human brain is intrinsically organized into dynamic, anticorrelated functional networks. *Proc. Natl. Acad. Sci. U.S.A.* 102, 9673–9678.
- Fox, M. D., and Raichle, M. E. (2007). Spontaneous fluctuations in brain activity observed with functional magnetic resonance imaging. *Nat. Rev. Neurosci.* 8, 700–711.
- Garrity, A. G., Pearlson, G. D., McKiernan, K., Lloyd, D., Kiehl, K. A., and Calhoun, V. D. (2007). Aberrant “default mode” functional connectivity in schizophrenia. *Am. J. Psychiatry* 164, 450–457.
- Geha, P. Y., Baliki, M. N., Harden, R. N., Bauer, W. R., Parrish, T. B., and Apkarian, A. V. (2008). The brain in chronic CRPS pain: abnormal gray-white matter interactions in emotional and autonomic regions. *Neuron* 60, 570–581.
- Guimera, R., and Amaral, L. A. N. (2005). Functional cartography of complex metabolic networks. *Nature* 433, 895–900.
- He, Y., Chen, Z., and Evans, A. (2008). Structural insights into aberrant topological patterns of large-scale cortical networks in Alzheimer’s disease. *J. Neurosci.* 28, 4756–4766.
- Jezzard, P., Mathews, P., and Smith, S. M. (2001). *Functional MRI: An Introduction to Methods*. Oxford: Oxford University Press.
- Laufs, H., Hamandi, K., Salek-Haddadi, A., Kleinschmidt, A., Duncan, J. S., and Lemieux, L. (2007). Temporal lobe interictal epileptic discharges affect cerebral activity in default mode brain regions. *Hum. Brain. Mapp.* 28, 1023–1032.
- Lui, S., Ouyang, L., Chen, Q., Huang, X., Tang, H., Chen, H., Zhou, D., Kemp, G. J., and Gong, Q. (2008). Differential interictal activity of the precuneus/posterior cingulate cortex revealed by resting state fMRI at 3T in generalized versus partial seizure. *J. Magn. Res. Imag.* 27, 1214–1220.
- May, A. (2008). Chronic pain may change the structure of the brain. *Pain* 137, 7–15.
- Meunier, D., Achard, S., Morcom, A., and Bullmore, E. T. (2009a). Age-related changes in modular organization of human brain functional networks. *Neuroimage* 44, 715–723.
- Meunier, D., Lambiotte, R., Fornito, A., Ersche, K., and Bullmore, E. T. (2009b). Hierarchical modularity in human brain functional networks. *Front. Neuroinform.* 3:37. doi: 10.3389/neuro.11.037.2009.
- Newman, M. E. J. (2004). Analysis of weighted networks. *Phys. Rev. E* 70, 056131–056139.
- Newman, M. E. J., and Girvan, M. (2004). Finding and evaluating community structure in networks. *Phys. Rev. E* 69, 026113–026127.
- Oshiro, Y., Quevedo, A. S., McHaffie, J. G., Kraft, R. A., and Coghill, R. C. (2009). Brain mechanisms supporting discrimination of sensory features of pain: a new model. *J. Neurosci.* 29, 14924–14931.
- PICA. <http://www.fmrib.ox.ac.uk/analysis/research/melodic>.

- Rand, W. M. (1971). Objective criteria for the evaluation of clustering methods. *J. Amer. Stat. Assoc.* 66, 846–850.
- Raichle, M. E., MacLeod, A. M., Snyder, A. Z., Powers, W. J., Gusnard, D. A., and Shulman, G. L. (2001). A default mode of brain function. *Proc. Natl. Acad. Sci. U.S.A.* 98, 676–682.
- Salvador, R., Suckling, J., Coleman, M. R., Pickard, J. D., Menon, D., and Bullmore, E. T. (2005). Neurophysiological architecture of functional magnetic resonance images of human brain. *Cereb. Cortex* 15, 1332–1342.
- Smith, S. M., Fox, P. T., Miller, K. L., Glahn, D. C., Fox, P. M., Mackay, C. E., Filippini, N., Watkins, K. E., Toro, R., Laird, A. R., and Beckmann, C. F. (2009). Close correspondence of major functional networks in rest and under task. *Proc. Natl. Acad. Sci. U.S.A.* 106, 13040–13045.
- Soranzo, N., Bianconi, G., and Altafini, C. (2007). Comparing association network algorithms for reverse engineering of large-scale gene regulatory networks: synthetic versus real data. *Bioinformatics* 23, 1640–1647.
- Sporns, O., Chialvo, D. R., Kaiser, M., and Hilgetag, C. C. (2004). Organization, development and function of complex brain networks. *Trends Cogn. Sci.* 8, 418–425.
- Stanberry, L., Murua, A., and Cordes, D. (2008). Functional connectivity mapping using the ferromagnetic Potts spin model. *Hum. Brain Mapp.* 29, 422–440.
- Tagliazucchi, E., Balenzuela, P., Fraiman, D., Chialvo, D. R. (2010). Brain resting state is disrupted in chronic back pain patients. *Neurosci. Lett.* 485, 26–31.
- Tracey, I., and Mantyh, P. W. (2007). The cerebral signature for pain perception and its modulation. *Neuron* 55, 377–391.
- Tzourio-Mazoyer, N., Landeau, B., Papathanassiou, D., Crivello, F., Etard, O., Delcroix, N., Mazoyer, B., and Joliot, M. (2002). Automated anatomical labeling of activations in SPM using a macroscopic anatomical parcellation of the MNI MRI single-subject brain. *Neuroimage* 15, 273–289.
- van den Heuven, M. P., Stam, C. J., Boersma, M., and Huisshof Pol, H. E. (2008). Small-world and scale-free organization of voxel-based resting-state functional connectivity in the human brain. *Neuroimage* 43, 528–539.
- Witting, N., Kupers, R. C., Svensson, P., Jensen, T. S. (2006). A PET activation study of brush-evoked allodynia in patients with nerve injury pain. *Pain* 120, 145–154.
- Zaki, J., Ochsner, K. N., Hanelin, J., Wager, T. D., and Mackey, S. C. (2007). Different circuits for different pain: Patterns of functional connectivity reveal distinct networks for processing pain in self and others. *Soc. Neurosci.* 2, 276–291.

Conflict of Interest Statement: The authors declare that the research was conducted in the absence of any commercial or financial relationships that could be construed as a potential conflict of interest.

Received: 26 February 2010; accepted: 18 October 2010; published online: 17 November 2010.

Citation: Balenzuela P, Chernomoretz A, Fraiman D, Cifre I, Sitges C, Montoya P and Chialvo DR (2010) Modular organization of brain resting state networks in chronic back pain patients. *Front. Neuroinform.* 4:116. doi: 10.3389/fninf.2010.00116

Copyright © 2010 Balenzuela, Chernomoretz, Fraiman, Cifre, Sitges, Montoya and Chialvo. This is an open-access article subject to an exclusive license agreement between the authors and the Frontiers Research Foundation, which permits unrestricted use, distribution, and reproduction in any medium, provided the original authors and source are credited.

APPENDIX

Table A1 | Cortical and subcortical regions in each hemisphere as defined in Tzourio-Mazoyer et al. (2002), abbreviations as in Salvador et al. (2005).

Region	Abbreviation
Precentral gyrus	PreCG
Superior frontal gyrus, dorsolateral	SFGdor
Superior frontal gyrus, orbital part	ORBSup
Middle frontal gyrus	MFG
Middle frontal gyrus, orbital part	ORBmid
Middle frontal gyrus, opercular part	IFGoperc
Inferior frontal gyrus, triangular part	IFGtriang
Inferior frontal gyrus, orbital part	ORBinf
Rolandic operculum	ROL
Supplementary motor area	SMA
Olfactory cortex	OLF
Superior frontal gyrus, medial	SFGmed
Superior frontal gyrus, medial orbital	ORBsupmed
Gyrus rectus	REC
Insula	INS
Anterior cingulate and paracingulate gyri	ACG
Median cingulate and paracingulate gyri	DCG
Posterior cingulate gyrus	PCG
Hippocampus	HIP
Parahippocampal gyrus	PHG
Amygdala	AMYG
Calcarine fissure and surrounding cortex	CAL
Cuneus	CUN
Lingual gyrus	LING
Superior occipital gyrus	SOG
Middle occipital gyrus	MOG
Inferior occipital gyrus	IOG
Fusiform gyrus	FFG
Postcentral gyrus	PoCG
Superior parietal gyrus	SPG
Inferior parietal, but supramarginal and angular gyri	IPL
Supramarginal gyrus	SMG
Angular gyrus	ANG
Precuneus	PCUN
Paracentral lobule	PCL
Caudate nucleus	CAU
Lenticular nucleus, putamen	PUT
Lenticular nucleus, pallidum	PAL
Thalamus	THAL
Heschl gyrus	HES
Superior temporal gyrus	STG
Temporal pole: superior temporal gyrus	TPOsup
Middle temporal gyrus	MTG
Temporal pole: middle temporal gyrus	TPOmid
Inferior temporal gyrus	ITG

Table A2 | List of regions composing each of the six communities found for the brain networks in each group.

Module name (Color, size)	HC
Visual (Red, 14)	CAL.L, CAL.R, CUN.L, CUN.R, LING.L, LING.R, SOG.L, SOG.R, MOG.L, MOG.R, IOG.L, IOG.R, FFG.L, FFG.R
Fronto-medial (Green, 22)	SFGdor.L, SFGdor.R, ORBSup.L, ORBSup.R, MFG.L, MFG.R, ORBmid.L, ORBmid.R, ORBInf.L, ORBInf.R, SFGmed.L, SFGmed.R, ORBSupmed.L, ORBSupmed.R, REC.L, REC.R, ACG.L, ACG.R, PCG.L, PCG.R, ANG.L, ANG.R
Parieto-temporal (Blue, 8)	PCUN.L, PCUN.R, MTG.L, MTG.R, TPOmid.L, TPOmid.R, ITG.L, ITG.R
Fronto-parietal (Light blue, 10)	IFGoperc.L, IFGoperc.R, IFGtriang.L, IFGtriang.R, SPG.L, SPG.R, IPL.L, IPL.R, SMG.L, SMG.R
Subcortical (Magenta, 16)	OLF.L, OLF.R, HIPL, HIPR, PHG.L, PHG.R, AMYG.L, AMYG.R, CAU.L, CAU.R, PUT.L, PUT.R, PAL.L, PAL.R, THA.L, THA.R
Sensorimotor (Yellow, 20)	PreCG.L, PreCG.R, ROL.L, ROL.R, SMA.L, SMA.R, INS.L, INS.R, DCG.L, DCG.R, PoCG.L, PoCG.R, PCL.L, PCL.R, HES.L, HES.R, STG.L, STG.R, TOPSup.L, TOPSup.R
Module name (Color, size)	CBP
Visual (Red, 16)	CAL.L, CAL.R, CUN.L, CUN.R, LING.L, LING.R, SOG.L, SOG.R, MOG.L, MOG.R, IOG.L, IOG.R, FFG.L, FFG.R, ITG.L, ITG.R
Fronto-medial (Green, 22)	SFGdor.L, SFGdor.R, MFG.L, MFG.R, IFGoperc.L, IFGoperc.R, IFGtriang.L, IFGtriang.R, SFGmed.L, SFGmed.R, ACG.L, ACG.R, PCG.L, PCG.R, SPG.L, SPG.R, IPL.L, IPL.R, ANG.L, ANG.R, PCUN.L, PCUN.R
Orbito-frontal (Blue, 12)	ORBSup.L, ORBSup.R, ORBmid.L, ORBmid.R, ORBInf.L, ORBInf.R, OLF.L, OLF.R, ORBSupmed.L, ORBSupmed.R, REC.L, REC.R
Fronto-parietal (Light blue, 12)	ROL.L, ROL.R, INS.L, INS.R, SMG.L, SMG.R, HES.L, HES.R, STG.L, STG.R, MTG.L, MTG.R
Subcortical (Magenta, 18)	HIPL, HIPR, PHG.L, PHG.R, AMYG.L, AMYG.R, CAU.L, CAU.R, PUT.L, PUT.R, PAL.L, PAL.R, THA.L, THA.R, TPOsup.L, TPOsup.R, TPOmid.L, TPOmid.R,
Sensorimotor (Yellow, 10)	PreCG.L, PreCG.R, SMA.L, SMA.R, DCG.L, DCG.R, PoCG.L, PoCG.R, PCL.L, PCR.R

The color code used to label each community in the figures is indicated as well

Healthy Controls

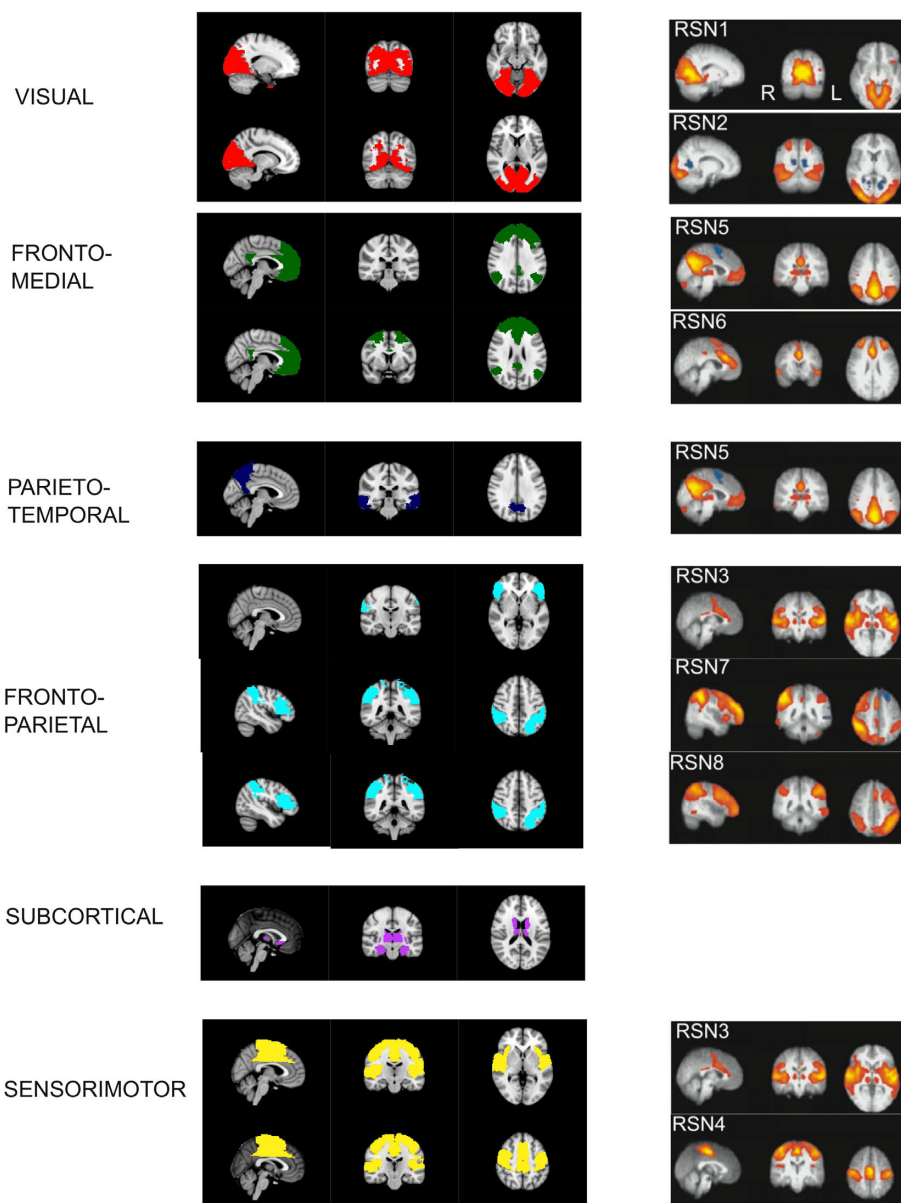
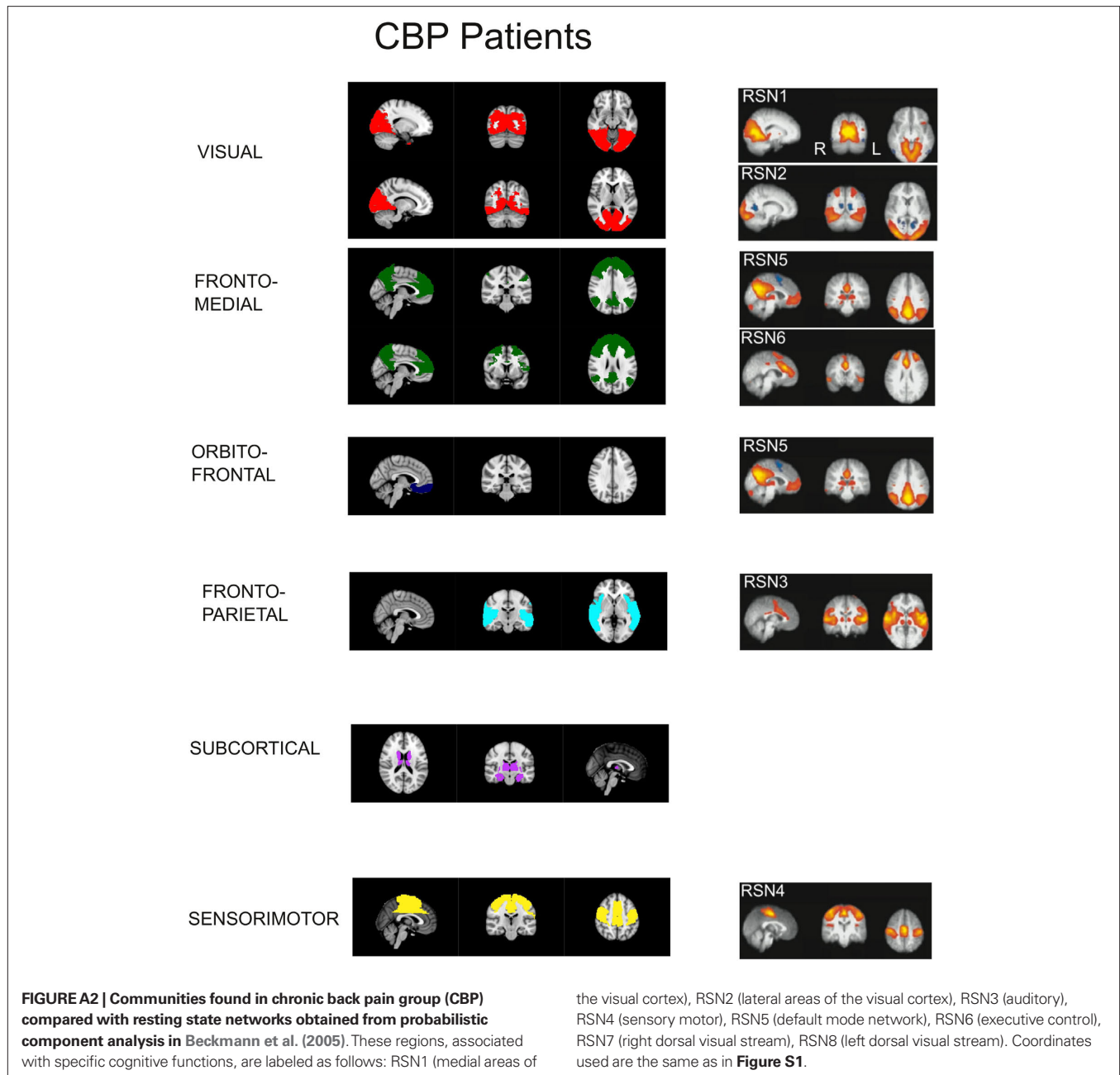


FIGURE A1 | Communities found in normal group (HC) compared with resting state networks obtained from probabilistic component analysis in Beckmann et al. (2005). These regions, associated with specific cognitive functions, are labeled as follows: RSN1 (medial areas of the visual cortex), RSN2 (lateral areas of the visual cortex), RSN3 (auditory), RSN4 (sensory motor), RSN5

(default mode network), RSN6 (executive control), RSN7 (right dorsal visual stream), RSN8 (left dorsal visual stream). Coordinates used are: RSN1, $x = 17$ $y = -73$ $z = -12$; RSN2, $x = -13$ $y = -61$ $z = 6$; RSN3: $x = 3$, $y = -17$, $z = 1.5$; RSN4, $x = 1$, $y = -21$, $z = 51$; RSN5, $x = -4$, $y = -29$, $z = 33$; RSN6, $x = 5$, $y = 6$, $z = 27$; RSN7, $x = 45$, $y = -42$, $z = 47$; RSN8, $x = -45$, $y = -42$, $z = 47$.



REFERENCES

Baliki, M. N., Chialvo, D. R., Geha, P. Y., Levy, R. M., Harden, R. N., Parrish, T. B., and Apkarian, A. V. (2006). Chronic pain and the emotional brain: specific brain activity associated with spontaneous fluctuations of intensity of chronic back pain. *J. Neurosci.* 26, 12165–12173.

Baliki, M. N., Geha, P. Y., Apkarian, A. V., and Chialvo, D. R. (2008). Beyond feeling: chronic pain hurts the brain, disrupting the default-mode network dynamics. *J. Neurosci.* 28, 1398–1403.

Fox, M. D., and Raichle, M. E. (2007). Spontaneous fluctuations in brain activity observed with functional

magnetic resonance imaging. *Nat. Rev. Neurosci.* 8, 700–711.

Salvador, R., Suckling, J., Coleman, M. R., Pickard, J. D., Menon, D., and Bullmore, E. T. (2005). Neurophysiological architecture of functional magnetic resonance images of human brain. *Cereb. Cortex* 15, 1332–1342.

Tzourio-Mazoyer, N., Landeau, B., Papathanassiou, D., Crivello, F., Etard, O., Delcroix, N., Mazoyer, B., and Joliot, M. (2002). Automated anatomical labeling of activations in SPM using a macroscopic anatomical parcellation of the MNI MRI single-subject brain. *Neuroimage* 15, 273–289.